UC San Diego

UC San Diego Electronic Theses and Dissertations

Title

Monitoring translation elongation from ribosome profiling data

Permalink

https://escholarship.org/uc/item/47h967t8

Author

Zhang, Jingxiao

Publication Date

2020

Peer reviewed|Thesis/dissertation

eScholarship.org Powered by the California Digital Library
University of California

UNIVERSITY OF CALIFORNIA SAN DIEGO

Monitoring Translation Elongation from Ribosome Profiling Data

A Thesis submitted in partial satisfaction of the requirements for the degree Master of Science

in

Biology

by

Jingxiao Zhang

Committee in Charge:

Professor Brian M. Zid, Chair
Professor Nan Hao, Co-Chair
Professor Steven Paul Briggs
Professor Scott Alan Rifkin
Professor James E Wilhelm

2020

Copyright

Jingxiao Zhang, 2020

All rights reserved.

The Thesis of Jingxiao Zhang is approved, and it is acceptable in quality and form for publication on microfilm and electronically:

Co-Chair

Chair

University of California San Diego

2020

DEDICATION

I dedicate this thesis to my grandfather for his infinite love and supports.

TABLE OF CONTENTS

LIST OF FIGURES

ACKNOWLEDGEMENT

I would like to thank Dr. Zid for accepting me working in his lab and being my committee chair. I also wish to thank Dr. Hao for leading me to the field of molecular biology and accepting to be my committee as well. Furthermore, I am also grateful to Dr. Rifkin, Dr. Briggs and Dr. Wilhelm who taught me how to present and kindly agreed to be on my committee.

I would like to thank A. Guzikowski and Dr. Zid for providing experiment data. I would like to thank all my lab members, their expertise, assistance, guidance, and patience throughout my time in the master program. Without your help, this thesis would not have been possible. It was great and enjoyable to work with you.

ABSTRACT OF THE THESIS

Monitoring Translation Elongation from Ribosome Profiling Data

by

Jingxiao Zhang

Master of Science in Biology

University of California San Diego, 2020

Professor Brian M. Zid, Chair
Professor Nan Hao, Co-Chair

Protein translation is regulated at the stages of initiation, elongation, and termination. Translation initiation has traditionally been thought of as the rate limiting step of translation under stresses. However, we find that during glucose starvation in yeast, differential translation elongation is a crucial mechanism that allows preferential translation of select genes during stress. While some growth mRNAs have similar overall ribosome occupancy compared to these upregulated stress mRNAs, their distribution of ribosomes is skewed towards the 3' end of the ORF. We also find that the skewed distribution in ribosomes during stress strongly correlates with increased mRNA

binding by the DEAD-box RNA helicase, Dhh1. We speculate the recruitment of Dhh1 is associated with this differential protein translation upon glucose starvation. By regulating translation through elongation, cells could more dynamically control protein synthesis under adverse conditions.

INTRODUCTION

Protein synthesis is regulated at all stages of translation: initiation, elongation and termination. The nutrient in growth medium controls the amount of protein synthesized. In the yeast Saccharomyces cerevisiae glucose-mediated pathway, depletion in glucose will lead to a general suppression of protein translation (Hinnebusch et al., 1984; Tzamarias et al., 1989; Rolfes and Hinnebusch, 1993). The initiation phase is generally considered as the rate-limiting step in the translation of an mRNA to protein, starting with the binding of ribosomes onto the 5' of gene transcripts. Previous study has been focused more on translation initiation as the key control step of translation across a variety of stresses, regulating the stress response at the level of protein (Ashe et al., 2000; Jackson & Pestova 2010). In the elongation step, the ribosome moves along the transcript bonding new amino acids to the amino acid chain by decoding each aminoacyl-tRNAs. Translation is terminated when the stop codon is reached and the translation process stops (Marshall et al., 2008; Livingstone et al., 2010). The translation-related rates could influence the abundance, structure and function of certain proteins produced by the cell. Understanding the role of initiation and elongation is important to decode the cellular regulation of gene expression (Borujeni and Salis, 2016; Kervestin and Amrani, 2004). It is therefore crucial to be able to accurately measure these rates.

With the technology of ribosome profiling, a deep-sequencing based quantitative tool, we are now able to extract these ribosome-protected mRNA fragments and align them to the yeast genome to monitor the translational process in yeast cells (Ingolia et al., 2009). These years, significant efforts were made to approximate these translation-related rates from data generated from ribosome profiling experiments. However, it is still hard to estimate elongation in stress

since the elongation and initiation rates are sometimes hard to differentiate in low read density profiling data.

DEAD-box RNA helicase, Dhh1 is presented in translational suppression and mRNA decay (Coller et al., 2001; Fischer and Weis, 2002; Presnyak and Coller, 2013), it has previously been considered as altering elongation rates based on codon optimality. Since mRNA decay is sensitive to the number of stalled ribosomes on the mRNA and the preferential binding of Dhh1 to low codon optimality mRNAs could block ribosome elongation, Dhh1 binding is considered as an indicative for slow ribosome movement, targeting slow translating mRNA and leading to decay (Radhakrishnan et al., 2016). Yet we find that the elongation stalling and Dhh1 recruitment was independent of the codons present in the mRNA. In glucose starvation, while both translation initiation and elongation are reduced, some growth mRNAs that are present pre-stress have similar levels of ribosomes present as those well-translated stress genes but minimal protein produced. We speculate the recruitment of Dhh1 is associated with this differential protein translation upon glucose starvation. We argued that although both translation initiation and elongation rate could reveal the level of translation suppression, Dhh1 enrichment enables differential translation elongation in genes that are essential to survival under stress, allowing preferential translation of these select genes. We will try to understand how translation elongation would change under different periods of stress and compare translation elongation rates among different transcripts. Furthermore, we will try to reveal the potential mechanism behind the differential translation elongation rates in yeast glucose starvation by examining the elongation rate in Dhh1 enriched genes compared to the elongation rate of other well translated genes presented pre-stress. Furthermore, we speculate that regulating translation through

elongation may allow cells to more dynamically control protein synthesis during adverse environmental conditions rather than relying on differential initiation.

RESULTS

Ribosome Occupancy doesn't correlate with initiation reads in glucose starvation.

To understand how translation is altered under different cell conditions, we use the ribosome profiling technology (Ingolia et al., 2009) to record the position of each ribosome protected mRNA fragments, which provide a genome-wide map of where the ribosomes are located and shifted between glucose-replete conditions and glucose-starvation conditions. We first examine the effect of glucose starvation on ribosome occupancy compared to logphase (Fig. 1A). Fold change of ribosome occupancy and mRNA level on individual genes were log2 transformed. In genes with mRNA levels increased during glucose starvation, we observed two classes of behavior: upregulated genes (log2(mRNA level fold change > 2.5)) also have increased ribosome occupancy compared to logphase, but the other group of genes that are also transcriptionally upregulated during glucose starvation experience a decrease in ribosome occupancy compared to logphase.

We further examine the effect of glucose starvation on ribosome footprint density among upregulated stress genes and pre-existing genes. The results agree with the previous experiments (Zid and O'Shea, 2014). In logphase, stress related genes like HSP30 have low ribosome occupancy whereas pre-existing genes like PAB1 have high ribosome occupancy (Fig. 1B). Ribosome occupancy level correlates with initiation reads, downstream ribosome distribution is also associated with accumulation of ribosomes around the start codon (Fig. 1C and Fig. 1D). In glucose starvation, pre-existing genes remain relatively highly associated with ribosomes similar to those upregulated stress genes (Fig. 1B). Those pre-existing genes have high ribosome

footprint density downstream but low initiation reads, whereas upregulated stress genes have high initiation rates but low downstream ribosome footprint density (Fig. 1E and Fig. 1F). Comparing the ribosome footprint densities of the two groups of genes in logphase and glucose starvation, we see differences in not only initiation reads but also the distribution of ribosome footprint density along the transcript.

3' end skewed distribution in ribosomes correlates with high Dhh1 binding in stress

In glucose starvation, mRNAs with high ribosome occupancy have different overall ribosome distributions. To quantify the differences in the ribosome footprints across transcripts, we computed a polarity score for every gene (Schuller et al., 2017). mRNAs with ribosomes skewed to the 3' end have greater polarity scores, whereas mRNAs with ribosomes skewed to the 5' end have lower polarity scores (Fig. 2A). With translation elongation shifting the ribosomes towards the 3' end, the distribution of ribosomes becomes more skewed towards the 3'end, resulting in a more positive polarity score. We examine the polarity scores in pre-existing mRNAs and those in upregulated stress mRNAs. Though the previous one has similar overall ribosome occupancy compared to these well-translated stress mRNAs, their distribution of ribosomes is skewed towards the 3' end of the ORF (Fig. 2B). We further examine the polarity scores shift in pre-existing mRNAs and upregulated stress mRNAs from logphase to glucose starvation. The pre-existing mRNAs experience a more positive polarity scores shift compared to the upregulated stress mRNAs. We also find that this skewed distribution of ribosomes in pre-existing mRNAs during glucose depletion strongly correlates with increased mRNA binding by the DEAD-box RNA helicase, Dhh1(Fig. 2C and Fig. 2D). Dhh1p has previously been implicated in altering elongation rates based on codon optimality, it couples translation to mRNA decay by sensing codon optimality (Radhakrishnan et al., 2016). Upregulated stress genes with

ribosome distribution more skewed towards 5' end experience a decreased Dhh1 binding during glucose depletion, whereas pre-existing genes have a more positive dhh1 enrichment score (Cary et al., 2015). In a longer glucose starvation period, Dhh1 enriched pre-existing mRNAs experience a less positive polarity scores shift compared to the upregulated stress mRNAs (Fig. 2E). In both ribosome polarity scores and polarity scores shift under glucose starvation, we see that Dhh1 enriched more in mRNAs with ribosomes distribution skewed to 3' end, also Dhh1 enriched more in mRNAs with high ribosome occupancy. Both results suggest that Dhh1 is recruited to pre-stress loaded ribosomes based on their overall distribution, thus slowing down elongation over time.

Translation elongation rate decreases in longer periods of Glucose starvation

Our understanding of the dynamics of protein translation was established based on a series of discrete time course information (Bostrom et al., 1986). We think using the time course ribosomes profiling data, we could infer the dynamic translation elongation by tracing the elongated ribosomes using ribosome profiling (Ingolia et al., 2009). We first let ribosomes to translate in the glucose repletion environment as our control case. We then allowed a period of time for run-off elongation and reduced initiation under a glucose depleted environment before we profile the ribosomes. We varied the time for run-off elongation to generate a set of ribosome footprints data (Fig 3A). These time course data could be assembled to provide us an insight of dynamic ribosome movement over a prolonged period of glucose depletion. In different glucose starvation periods, we observed a transcriptome-wide increase in polarity scores, which indicates ribosome elongation from 5'end to 3'end. We also observed that polarity scores shift become less positive over a longer period of glucose depletion (Fig. 3B). Metagene analysis on ribosome footprint density across the transcriptome revealed a progressive depletion of ribosomes from the

5′ to the 3′ of the transcriptome under glucose depletion (Fig. 3C). The elongation rate under each time period of stress is measured by three different methods. All three methods produce decreased elongation rates with longer stress periods (Fig. 3D and Fig. 3E). The shift distance in ribosome footprint density reduced over time. Translation elongation efficiency reduced overtime, for a relative ribosome density within a certain range of codon to reduce to 0, the average amount of time needed increased under longer glucose depletion period. In the change of elongation rate (Fig 3E), we also find that compared to the elongation rate in the first minute, translation elongation rate decreased the most in the first 5 minutes of glucose depletion. After 5 minutes, there's not much decrease in elongation rate compared to the previous one.

Enrichment of Dhh1 alters elongation rates on well translated mRNAs

We find that the skewed distribution of ribosomes in pre-existing mRNAs during glucose depletion strongly correlates with increased mRNA binding of Dhh1. In our time course data, we measured the Dhh1 binding under stress and the calculated elongation. We select the well translated mRNAs in logphase according to the averaged ribosome footprint density per codon. The Dhh1 enriched mRNAs are selected based on the change in Dhh1 binding from logphase to glucose depletion (Cary et al., 2015). The mechanism of Dhh1 binding and ribosome elongation rates are shown in (Fig 4A). With an increased amount of Dhh1 bound to a well translated mRNA, more ribosomes are stalled and are not able to elongate along the transcript. We find that the enrichment of Dhh1 under a prolonged glucose starvation period could alter the elongation rate on the well translated mRNAs (Fig 4B). We then compare the change in elongation rate over a longer glucose depletion period. By calculating the relative elongation rates in 5 minutes and 15 minutes to the first minute of glucose starvation, we find that the average run-off of ribosomes on Dhh1 enriched genes are reduced faster in the longer stress periods, compared to

the average run-off on all genes (Fig 4C). Also, translation elongation efficiency reduced faster in these genes over longer depletion time (Fig 4D). Although the first minute depletion elongation rate in Dhh1 enriched genes is higher than the average in all genes, the decrease in elongation rate in 5 minutes and 15 minutes is also higher.

DISCUSSION

A common response, essential to cellular survival during adverse environmental conditions, is the suppression of overall translation during stress. Previous study has shown glucose depletion rapidly inhibits translation initiation (Ashe et al., 2000) and role of initiation versus elongation in regulating protein production are still actively debated (Tuller et al., 2010a; Gingold and Pilpel, 2011; Chu et al., 2011). Understanding how translation elongation is regulated in relation to protein production is important, as changes in the amount of protein synthesis can lead to both cancers and the overall aging process (Truitt and Ruggero, 2017; McCormick et al., 2015; Steffen et al., 2008). Few studies focused on translation elongation control under stress, translation initiation has traditionally been thought of as the key control step of translation across a variety of stresses (Ashe et al., 2000). We find that during glucose starvation in yeast, both pre-existing genes and upregulated stress genes have high ribosome occupancy, but pre-existing genes produce minimal amounts of protein compared to the upregulated stress genes. If on each mRNA, ribosomes are not stalled, proteins should be synthesized at the rate which correlates with the number of new mRNA produced times the number of ribosomes initiated per mRNA (Riba et al., 2019). Yet we find that ribosome initiation reads do not correlate with the amount of protein synthesized in glucose starvation. Translation initiation is not the only key control step in translation under glucose starvation, differential

translation elongation is also a crucial mechanism that allows preferential translation of select genes during stress.

Ribosome profiling technology records the position of a translating ribosome by using the fact that ribosomes protect discrete footprints on the mRNA templates from nuclease digestion (Ingolia et al., 2009). With ribosome profiling data, we are able to examine the ribosome footprint density and the overall distribution of ribosome reads. Polarity scores quantify ribosomes distribution by comparing the ratio of enrichment on the 5' and 3’ side of a transcript, providing us an insight of how translation elongation shifts ribosome distribution in glucose depletion. Over a prolonged stress period, the polarity peak gradually shifted from shorter genes to longer genes, and the change in polarity scores decreased (Fig. 3B). This polarity scores shift suggests that shorter genes might be easier to lose ribosomes compared to longer genes due to their length. However, given that we estimate a transcriptome-wide average, we assume all the ribosomes at the same time point are moving at the same speed on mRNAs. Although elongation rates are different among genes but the transcriptome-wide elongation slows down in glucose depletion. However, polarity cannot measure the distance in ribosome shift, it only indicates the ratio not the actual ribosomes number. Here we present three different methods, based on the position of ribosome-protected fragments, that could help expand our ability to define the range of ribosome movement and determine the transcriptome-wide average elongation rate.

We estimate translation elongation rate by applying a pulse-chase ribosome profiling strategy (Ingolia et al., 2011), all three calculations show that compared to the ribosome footprint density at logphase, glucose depletion causes a progressive depletion of ribosomes from the 5′ to the 3′ of the transcriptome. The calculated elongation rates drop rapidly after the first minute of glucose starvation (Fig. 3E). Since translation initiation is reduced rapidly under stress, most

polysomes were lost in the first minute of stress, an indicative of an inhibition of initiation (Ashe et al., 2000). This delayed reaction of elongation rate compared to initiation under stress might suggest that elongation might be the key control step of translation repression under a prolonged glucose depletion period. The slowing down of translation elongation, coupled with a reduced initiation rate under glucose starvation, allows the cells to suppress overall translation under adverse environment.

Although translation is globally suppressed during glucose starvation, some stress response genes are preferentially translated to deal with stress conditions (Zid and O'Shea, 2014). We speculate that Dhh1 is recruited to pre-stress loaded ribosomes, regulating translation through elongation. Recruitment of Dhh1 caused a change in elongation rate on well translated mRNAs. If we examine the elongation rate of Dhh1 enriched mRNAs, these mRNAs actually have a larger elongation rate in the first minute of glucose depletion (Fig 4B). Since the inhibition of elongation is not as fast as that of initiation and the binding of Dhh1 might take some time. We think the change in elongation rate after the first minute is more significant than the change in the first minute. Like other well translated mRNAs, the Dhh1 enriched mRNAs also experience a dramatic drop in elongation rate between the first minute and five minutes of glucose starvation, but the elongation rates of Dhh1 enriched mRNAs decrease much faster. This huge drop in elongation rates after the first minute of stress indicates that Dhh1 binding gradually stalled ribosomes on mRNAs, causing a more dramatic change in elongation.

METHODS

Ribosome footprint data

In the pulse-chase experiment we did, yeast cells were treated under glucose starvation for 1 minutes, 5 minutes and 15 minutes. The ribosome protected fragments were sequenced and

the resulting ribosome profiling data were used to estimate the time course translation elongation rates.

Analysis of ribosome profiling and RNA sequencing data

PolyA tails were trimmed off from the sequences, the trimmed fragments were then sent to bowtie Aligner. After removing reads mapping to non-coding RNA, reads were mapped to S. cerevisiae reference genome R64-1-1 using bowtie (Langmead et al., 2009). The aligned reads were counted and sorted with yeast coding sequence, extracted features into Excel compatible files. In RNA-Seq data, the mRNA levels were normalized by FPKM. Ribo-Seq and RNA-Seq data analysis was performed using a customized analysis pipeline written in Python3, available in GitHub at https://github.com/jiz225/Zid-Lab/tree/master/Sequence%20analysis.

Next we calculate ribosome occupancy for each gene. The ribosome occupancy was calculated by the total ribosome reads from ribosome profiling divided by mRNA level in FPKM. The change in ribosome occupancy and mRNA level were log2 transformed and visualized with Python. Genes were then grouped by stress induced ribosome occupancy fold change and mRNA level fold change. Upregulated high ribosome occupancy genes were selected with ribosome occupancy fold change > 0 and mRNA level fold change > 2.5. Upregulated low ribosome occupancy genes were selected with ribosome occupancy fold change < -1 and mRNA level fold change > 2.5.

Polarity Score Calculation

The first 15 bp of the coding sequence were excluded when quantifying the ribosome distribution on a mRNA. The start site was shifted by 15 bp and from the start site we calculated a cumulative polarity score by position. The polarity at position i in a gene of length l is defined as follows: $p_{\mathrm{i}} = \frac{d_{\mathrm{i}} w_{\mathrm{i}}}{\sum_{i=1}^{l} d_{\mathrm{i}}}$, where $w_{\mathrm{i}} = \frac{2i - (l+1)}{l-1}$

The terms d_i is the ribosome footprint and w_i is the relative distance from position i to the center of the gene. Polarity score for a gene is the total sum of p_i for all positions i within the ORF (Schuller et al., 2017). The polarity shift under stress is defined by the difference in gene polarity score from logphase to glucose starvation. The shift in gene polarity score from pulse-chase experiment was plotted against the gene length and averaged by a 30bp sliding window. Python was used to visualize peak polarity shifts across the transcriptome.

Constructing metagene Profiles

Mean footprint densities were calculated in all coding sequences, excluding the first 15 bp. A non-overlapped five-codon sliding window was used to measure the average read per window along the coding sequence and well-translated genes were selected based on a mean value of at least 1 read per window in the logphase sample (Ingolia et al., 2011). Then we construct the metagene profiles in 1 minute, 5 minutes and 15 minutes of glucose starvation data. In each gene, ribosome footprint density at each read position was then normalized by the average ribosome footprint density of all the footprint positions on that transcript. With the average density normalization, we reduce the biased effect caused by low ribosome footprint density. With the goal of being more robust in comparing samples with ribosomes mostly run-off and those with ribosomes mostly stalled, we further normalize the metagene profiles across samples using median ratio normalization. Which brings the median of the samples closer and reduces variance between genes for the following calculation.

Translational Elongation Calculations

The range of ribosome runoff caused by glucose starvation was the region between initiation end site and depletion end site. Initiation end site is the last codon position with ribosomes accumulated due to translation initiation, depletion end site is the last codon position

with ribosomes depleted compared to the ribosomes density of logphase. We assume there is no initiation take place or elongation is not affected by initiation rate after this initiation end site and no more ribosome runoff after the depletion end site. Each metagene profile constructed by glucose starvation data has its depletion end site. The depletion end site was estimated by taking the difference between stress and logphase profiles and finding the first codon position with at least 50% of the 20 ribosome reads following it are not lower than those of logphase. There are three ways of translation elongation estimation. Peak movement calculation is taking the difference of depletion end site in two different glucose starvation profiles, which represent the distance of continued runoff after the depletion end site of the first glucose starvation profile.

Ribosome footprint shift captures the codon position with similar (≥0.01) ribosome footprint density from two different glucose starvation profiles and gets the distance between them, then computes the average of all the distances. Translation efficiency estimation quantifies the depletion of ribosome density across the transcriptome as a function of time (Sharma et al., 2019). Ribosome $\rho(t = \Delta t, L)$ with Δt = duration of glucose starvation in minutes, of individual metagene profile is calculated by taking the average of all ribosome densities within the range (0, L) for different L. The ribosome density of logphase is denoted $\rho(t = 0, L)$. For metagene profiles of glucose starvation, we calculated relative ribosome density $\frac{p(t=\Delta t,L)}{\rho(t=0,L)}$, $\frac{p(t=\Delta t,L)}{\rho(t=0,L)} = 1 - \frac{dL}{d\tau(L)}$ where $\tau(L)$ is the average time at which $\frac{p(t=\Delta t,L)}{\rho(t=0,L)}$ *e*quals zero, the average time needed for the ribosomes to move from codon position 0 to L. We plot L against $\tau(L)$, transcriptome averaged elongation is $\frac{dL}{d\tau(L)}$. The estimated translation elongation of the three methods are compared in all three time courses: 1 minute, 5 minutes and 15 minutes of glucose starvation. Change in elongation rate is measured by $\frac{Elongation\ rate\ of\ \ \Delta t\ \ minute\ stress}{Elongation\ rate\ of\ First\ minute\ stress}$.

FIGURES

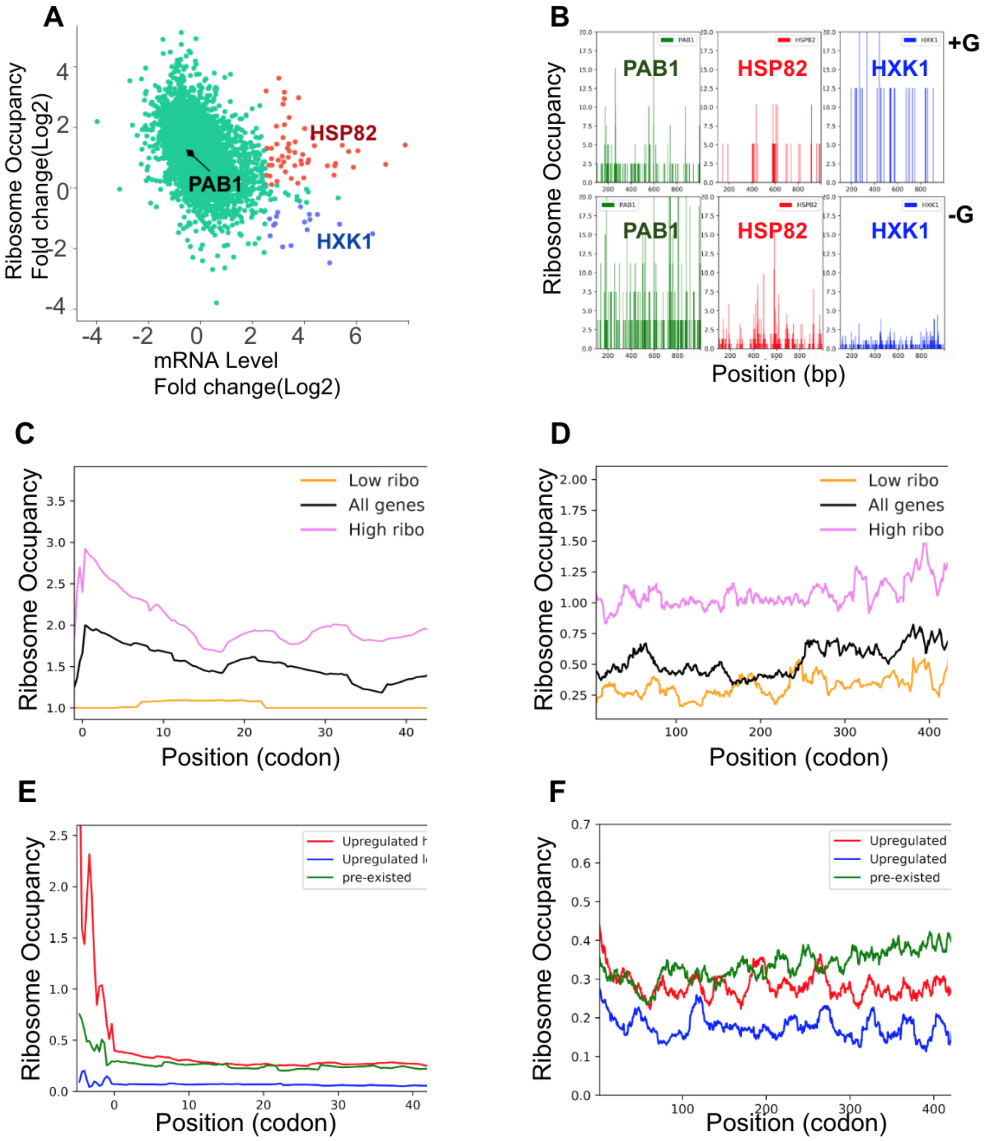

Figure 1: Ribosome Occupancy doesn't correlate with initiation reads in glucose starvation. (A) Glucose depletion changes gene specific mRNA level and ribosome occupancy. The $\log_2$ fold-changes of ribosome occupancy versus $\log_2$ fold-changes of mRNA level in all genes are shown. (B) Gene specific ribosome occupancy of differentially regulated genes in glucose starvation. Ribosome occupancy numbers along the gene transcript of *HSP30*, *PAB1* and *HXK1* are shown to compare logphase and glucose depletion. (C-D) Ribosome initiation reads and downstream ribosome occupancy distribution in logphase. Low ribosome occupancy genes, all genes and high ribosome occupancy genes are shown. (E-F) Ribosome initiation reads and downstream ribosome occupancy distribution in glucose depletion. Initiation reads and downstream ribosome distributions of upregulated low ribosome occupancy genes, pre-existing genes and upregulated high ribosome occupancy genes.

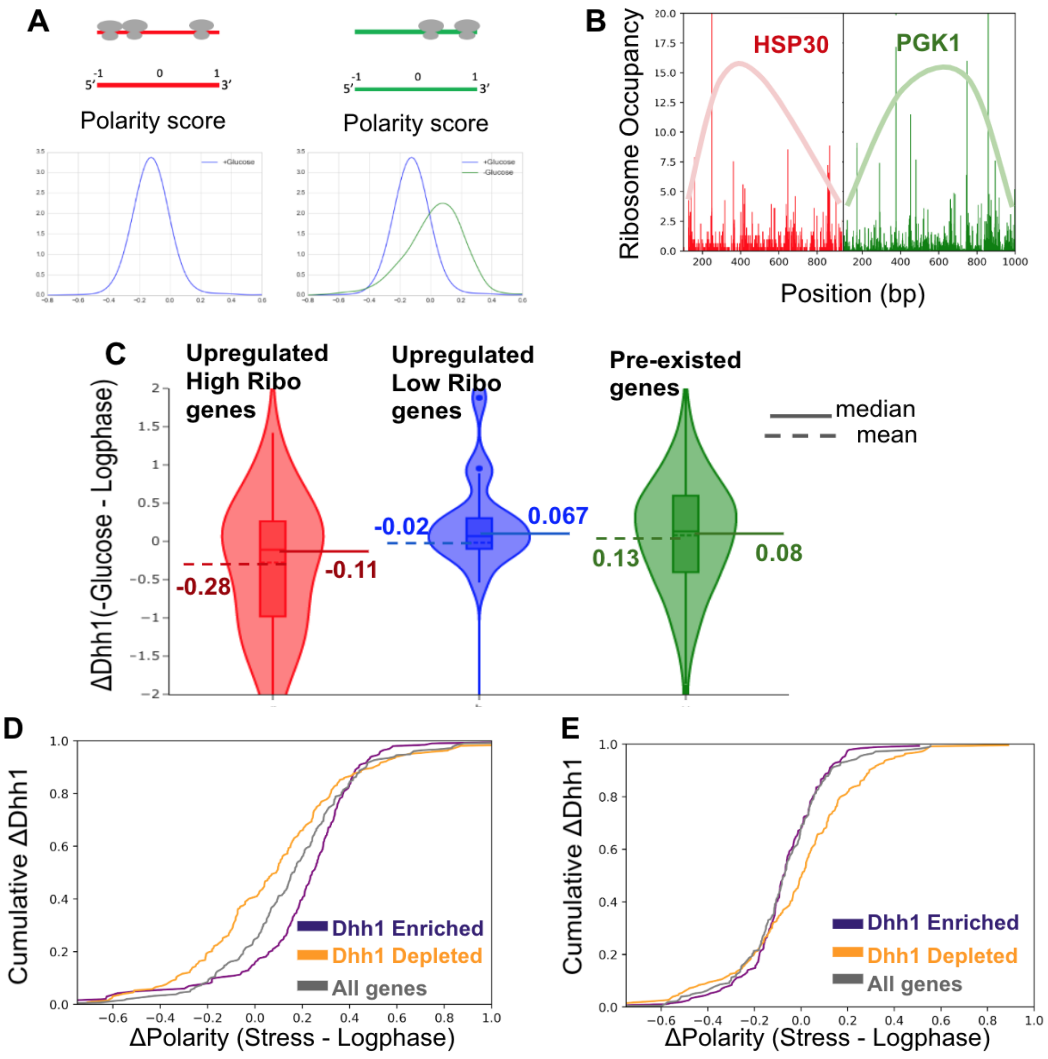

Figure 2: 3' end skewed ribosome distribution correlates with high Dhh1 binding in stress. (A) Schematic of polarity score. (B) Ribosome distribution along the gene transcript in glucose depletion. Ribosome distributions of upregulated stress gene *HSP30* and pre-existing gene *PGK1* are compared, both of them have high ribosome occupancy in glucose depletion. (C) Dhh1 recruitment in glucose starvation in differentially regulated genes. The median and mean of Dhh1 enrichment scores are shown in each group of genes. (D-E) Gene specific polarity scores change and the ability to recruit Dhh1 under glucose starvation. The change in polarity scores from logphase to glucose starvation are shown with cumulative Dhh1 binding in high Dhh1 binding genes, low Dhh1 binding genes and all genes. The polarity scores change under 7.5 minutes of glucose starvation and under 15 minutes of glucose starvation are shown.

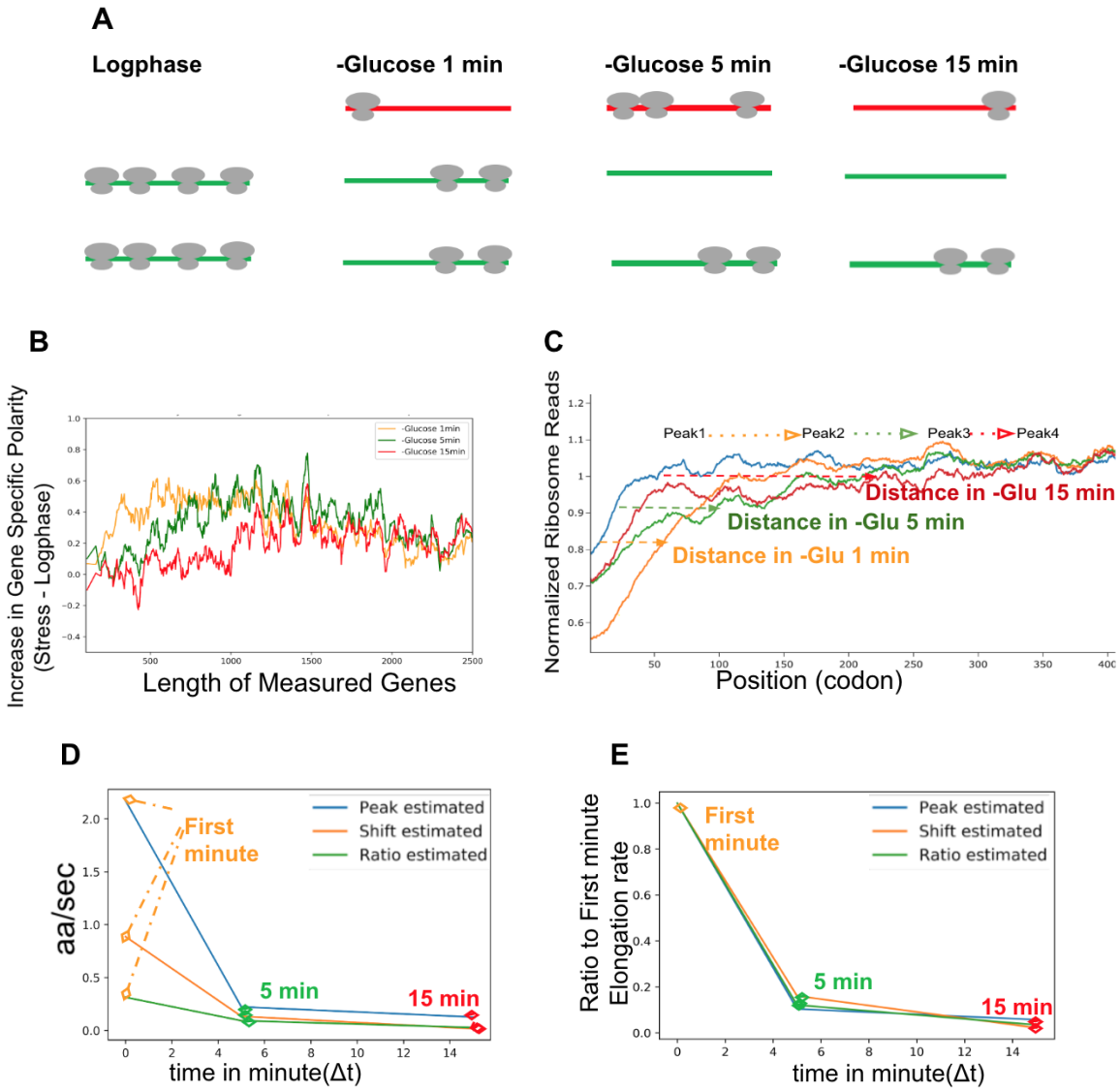

Figure 3: Translation elongation rate decreases in longer periods of Glucose starvation. (A) Schematic of ribosome run-off. (B) Gene specific polarity scores change under different time periods of glucose starvation. The polarity score under each glucose starvation period is compared with the polarity score in logphase, gene specific polarity scores are sorted by the genes length. (C) Metagene analysis of ribosome run-off elongation. Ribosome footprint density was averaged across 10 codon sliding windows for samples treated with different glucose starvation time. (D) Estimated rate of ribosome elongation. Elongation rates estimated by three different methods are shown in each run-off period. (E) Relative elongation rate compared to first minute of glucose depletion.

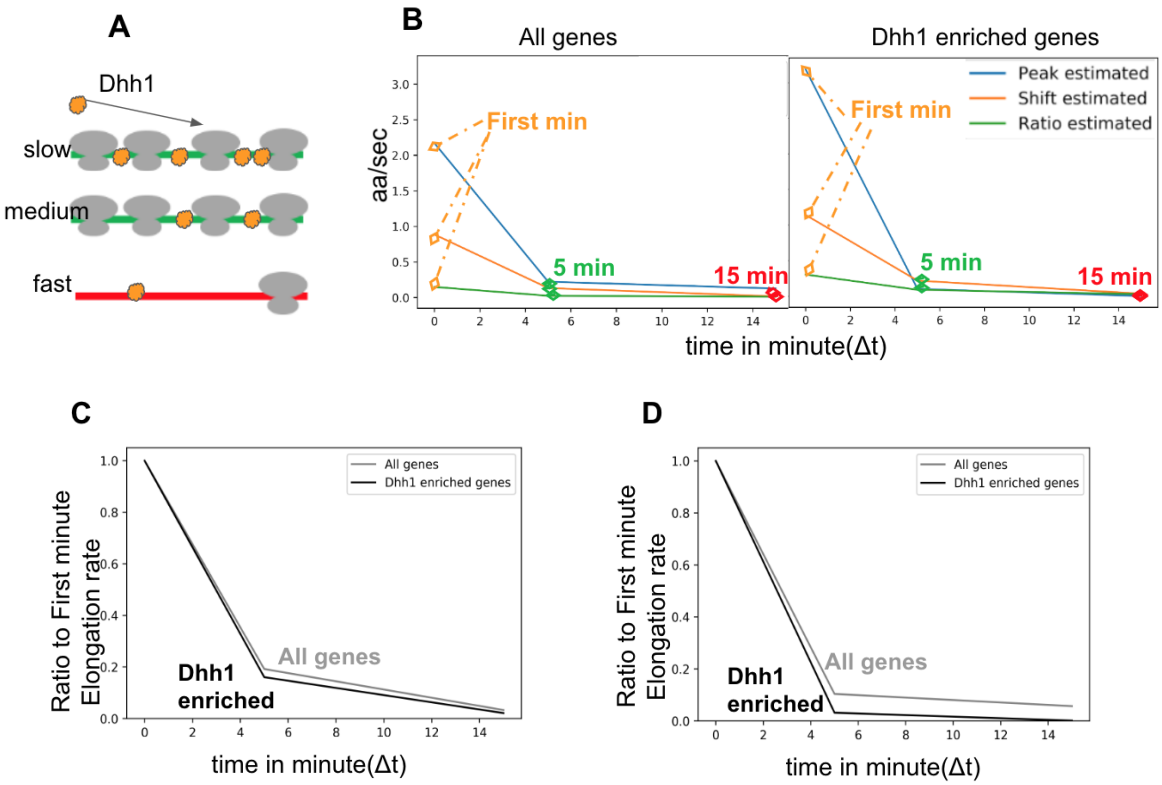

Figure 4: Enrichment of Dhh1 alters elongation rates on well translated mRNAs. (A) Dhh1 binding and ribosome elongation rate. (B) Estimated average elongation rate in Dhh1 enriched genes and all genes. (C) Relative elongation rate compared to the first minute of glucose depletion estimated by the shift distance in ribosome reads. The average in Dhh1 enriched genes and in all genes are shown. (D) Relative elongation rate compared to the first minute of glucose depletion estimated by translation elongation efficiency. The average in Dhh1 enriched genes and in all genes are shown.

REFERENCES

Ashe, M. P., De Long, S. K., & Sachs, A. B. (2000). Glucose depletion rapidly inhibits translation initiation in yeast. Molecular biology of the cell, 11(3), 833–848. https://doi.org/10.1091/mbc.11.3.833

Bostrom, K., Wettesten, M., Boren, J., Bondjers, G., Wiklund, O., Olofsson, S. O. (1986). Pulse-chase studies of the synthesis and intracellular transport of apolipoprotein B-100 in HepG2 cells. The Journal of biological chemistry.261:13800–13806.

Cary, G. A., Vinh, D. B., May, P., Kuestner, R., & Dudley, A. M. (2015). Proteomic Analysis of Dhh1 Complexes Reveals a Role for Hsp40 Chaperone Ydj1 in Yeast P-Body Assembly. G3 (Bethesda, Md.), 5(11), 2497–2511. https://doi.org/10.1534/g3.115.021444

Chu, D., & von der Haar, T. (2012). The architecture of eukaryotic translation. Nucleic acids research, 40(20), 10098–10106. https://doi.org/10.1093/nar/gks825

Coller, J. M., Tucker, M., Sheth, U., Valencia-Sanchez, M. A., & Parker, R. (2001). The DEAD box helicase, Dhh1p, functions in mRNA decapping and interacts with both the decapping and deadenylase complexes. RNA (New York, N.Y.), 7(12), 1717–1727. https://doi.org/10.1017/s135583820101994x

Espah Borujeni, A. and Salis, H. M. (2016). Translation initiation is controlled by rna folding kinetics via a ribosome drafting mechanism. Journal of the American Chemical Society, 138(22):7016–7023. https://doi.org/10.1021/jacs.6b01453

Fischer, N., & Weis, K. (2002). The DEAD box protein Dhh1 stimulates the decapping enzyme Dcp1. The EMBO journal, 21(11), 2788–2797. https://doi.org/10.1093/emboj/21.11.2788

Gingold, H., & Pilpel, Y. (2011). Determinants of translation efficiency and accuracy. Molecular systems biology, 7, 481. https://doi.org/10.1038/msb.2011.14

Hinnebusch A. G. (1984). Evidence for translational regulation of the activator of general amino acid control in yeast. Proceedings of the National Academy of Sciences of the United States of America, 81(20), 6442–6446. https://doi.org/10.1073/pnas.81.20.6442

Ingolia, N. T., Ghaemmaghami, S., Newman, J. R., & Weissman, J. S. (2009). Genome-wide analysis in vivo of translation with nucleotide resolution using ribosome profiling. Science (New York, N.Y.), 324(5924), 218–223. https://doi.org/10.1126/science.1168978

Ingolia, N. T., Lareau, L. F., & Weissman, J. S. (2011). Ribosome profiling of mouse embryonic stem cells reveals the complexity and dynamics of mammalian proteomes. Cell, 147(4), 789–802. https://doi.org/10.1016/j.cell.2011.10.002

Jackson, R., Hellen, C. & Pestova, T. (2010). The mechanism of eukaryotic translation initiation and principles of its regulation. Nat Rev Mol Cell Biol 11, 113–127 https://doi.org/10.1038/nrm2838

Kervestin, S., & Amrani, N. (2004). Translational regulation of gene expression. Genome biology, 5(12), 359. https://doi.org/10.1186/gb-2004-5-12-359

Langmead, B., Trapnell, C., Pop, M., and Salzberg, S. L. (2009). Ultrafast and memory-efficient alignment of short dna sequences to the human genome. Genome Biology,10(3):R25. https://doi.org/10.1186/gb-2009-10-3-r25

Livingstone, M., Atas, E., Meller, A. & Sonenberg, N. (2010). Mechanisms governing the control of mRNA translation, Physical Biology 7, no. 2, 021001. https://doi.org/10.1088/1478-3975/7/2/021001

Marshall, R. A., Aitken, C. E., Dorywalska, M., and Puglisi, J. D. (2008). Translation at the single-molecule level. Annual Review of Biochemistry, 77(1):177–203. PMID: 18518820. https://doi.org/10.1146/annurev.biochem.77.070606.101431

McCormick, M. A., Delaney, J. R., Tsuchiya, M., Tsuchiyama, S., Shemorry, A., Sim, S., Chou, A. C., Ahmed, U., Carr, D., Murakami, C. J., Schleit, J., Sutphin, G. L., Wasko, B. M., Bennett, C. F., Wang, A. M., Olsen, B., Beyer, R. P., Bammler, T. K., Prunkard, D., Johnson, S. C., … Kennedy, B. K. (2015). A Comprehensive Analysis of Replicative Lifespan in 4,698 Single-Gene Deletion Strains Uncovers Conserved Mechanisms of Aging. Cell metabolism, 22(5), 895–906. https://doi.org/10.1016/j.cmet.2015.09.008

Presnyak, V., & Coller, J. (2013). The DHH1/RCKp54 family of helicases: an ancient family of proteins that promote translational silencing. Biochimica et biophysica acta, 1829(8), 817–823. https://doi.org/10.1016/j.bbagrm.2013.03.006

Radhakrishnan, A., Chen, Y. H., Martin, S., Alhusaini, N., Green, R., & Coller, J. (2016). The DEAD-Box Protein Dhh1p Couples mRNA Decay and Translation by Monitoring Codon Optimality. Cell, 167(1), 122–132.e9. https://doi.org/10.1016/j.cell.2016.08.053

Riba, A., Di Nanni, N., Mittal, N., Arhn´e, E., Schmidt, A., and Zavolan, M. (2019). Protein synthesis rates and ribosome occupancies reveal determinants of translation elongation rates. Proceedings of the National Academy of Sciences, 116(30):15023. https://doi.org/10.1073/pnas.1817299116

Rolfes, R. J., & Hinnebusch, A. G. (1993). Translation of the yeast transcriptional activator GCN4 is stimulated by purine limitation: implications for activation of the protein kinase GCN2. Molecular and cellular biology, 13(8), 5099–5111. https://doi.org/10.1128/mcb.13.8.5099

Schuller, A. P., Wu, C. C., Dever, T. E., Buskirk, A. R., & Green, R. (2017). eIF5A Functions Globally in Translation Elongation and Termination. Molecular cell, 66(2), 194–205.e5. https://doi.org/10.1016/j.molcel.2017.03.003

Sharma, A.K., Sormanni, P., Ahmed, N., Ciryam, P., Friedrich, U.A., Kramer, G., O'Brien, E.P. (2019). A chemical kinetic basis for measuring translation initiation and elongation rates from ribosome profiling data. PLoS Computational Biology, 15(5), art. no. e1007070. https://doi.org/10.1371/journal.pcbi.1007070

Steffen, K. K., MacKay, V. L., Kerr, E. O., Tsuchiya, M., Hu, D., Fox, L. A., Dang, N., Johnston, E. D., Oakes, J. A., Tchao, B. N., Pak, D. N., Fields, S., Kennedy, B. K., & Kaeberlein, M. (2008). Yeast life span extension by depletion of 60s ribosomal subunits is mediated by Gcn4. Cell, 133(2), 292–302. https://doi.org/10.1016/j.cell.2008.02.037

Truitt, M. L., & Ruggero, D. (2016). New frontiers in translational control of the cancer genome. Nature reviews. Cancer, 16(5), 288–304. https://doi.org/10.1038/nrc.2016.27

Tuller, T., Carmi, A., Vestsigian, K., Navon, S., Dorfan, Y., Zaborske, J., Pan, T., Dahan, O., Furman, I., Pilpel, Y. (2010). An evolutionarily conserved mechanism for controlling the efficiency of protein translation. Cell 141:344–354. ttps://doi.org/10.1016/j.cell.2010.03.031

Tzamarias D., Roussou I., Thireos G. (1989). Coupling of GCN4 mRNA translational activation with decreased rates of polypeptide chain initiation. Cell 57, 947-954. https://doi.org/10.1016/0092-8674(89)90333-4

Zid, B., O'Shea, E. (2014). Promoter sequences direct cytoplasmic localization and translation of mRNAs during starvation in yeast. Nature 514, 117–121. https://doi.org/10.1038/nature13578